

# Crack-Length Determination for the Compact Tension Specimen Using a Crack-Opening- Displacement Calibration – Comparison of COD Measured Graphically and From the Gage Output

A. M. SULLIVAN

*Strength of Metals Branch  
Engineering Materials Division*

December 10, 1975



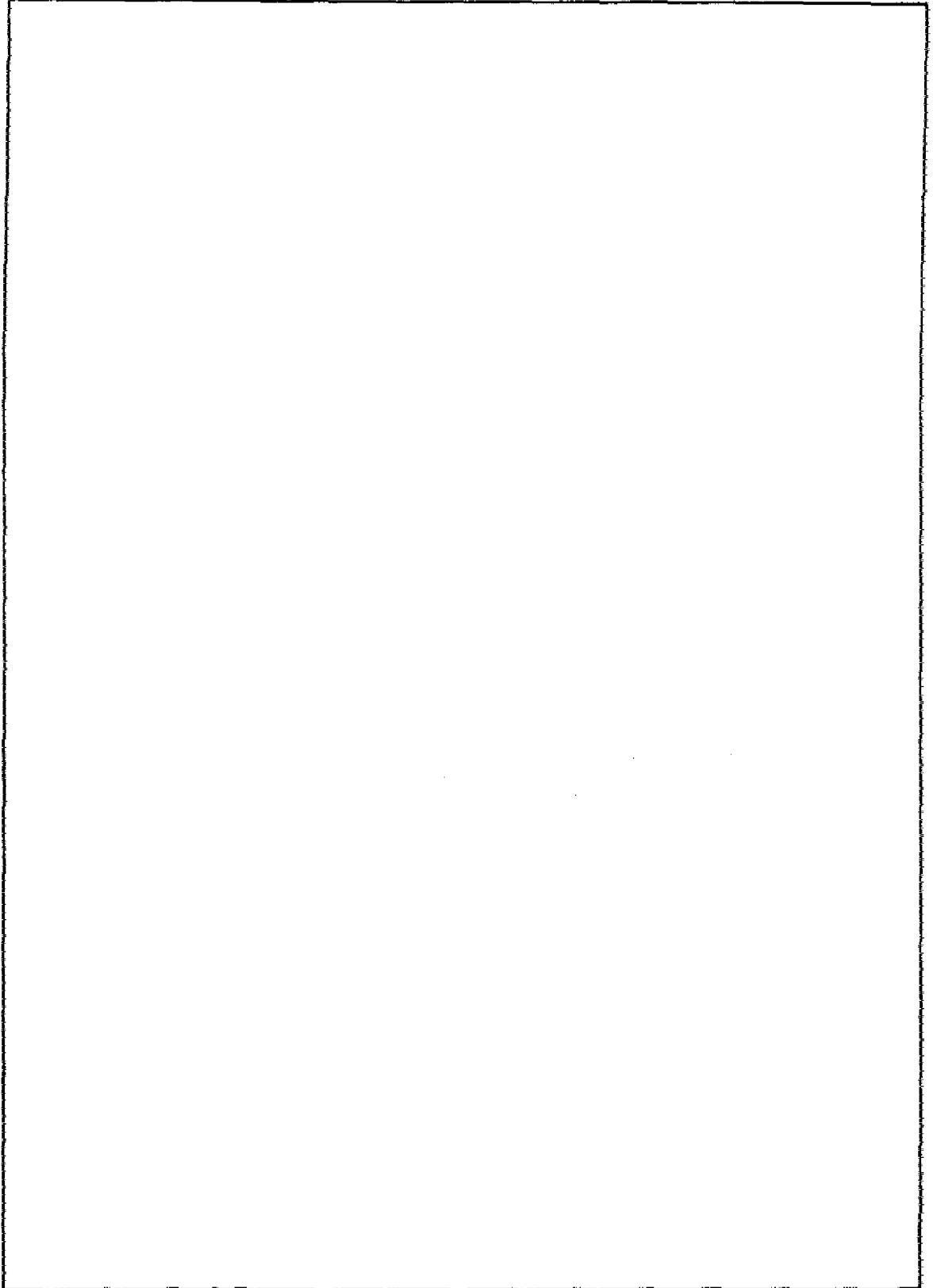
**NAVAL RESEARCH LABORATORY**  
Washington, D.C.

Approved for public release; distribution unlimited. *DDC-A*



UNCLASSIFIED

SECURITY CLASSIFICATION OF THIS PAGE(When Data Entered)



UNCLASSIFIED

SECURITY CLASSIFICATION OF THIS PAGE(When Data Entered)

## CONTENTS

SYMBOLS .....	iv
INTRODUCTION .....	1
EXPERIMENTAL CONSIDERATIONS .....	2
Material .....	2
Specimen Geometry .....	3
Test Procedure .....	3
Data Reduction .....	4
DISCUSSION OF EXPERIMENTAL RESULTS .....	5
CONCLUSIONS .....	13
ACKNOWLEDGMENT .....	13
REFERENCES .....	13

## SYMBOLS

a	Total crack length of a CT specimen measured from the load point
$a_{COD}$	Crack length measured graphically
$a_{mv}$	Crack length determined from mv readings
a/W	Crack length-to-width ratio
B	Specimen thickness
COD	Crack-opening displacement
CT	Compact tension specimen
da/dN	Crack-growth rate; change in length per cycle
E	Young's modulus
FCGR	Fatigue crack-growth rate
h	Specimen half height
$\Delta K$	Stress-intensity-factor range
$\Delta K_{eff}$	Stress-intensity-factor range corrected for the effect of stress ratio R
P	Load
N	Number of cycles
R	Stress ratio; $\sigma_{min}/\sigma_{max}$
$\sigma$	Stress
W	Specimen width

CRACK-LENGTH DETERMINATION FOR THE COMPACT TENSION SPECIMEN  
USING A CRACK-OPENING-DISPLACEMENT CALIBRATION --  
COMPARISON OF COD MEASURED GRAPHICALLY  
AND FROM THE GAGE OUTPUT

## INTRODUCTION

Development of verified and documented procedures for materials testing is an on-going process of importance to the Navy. New experimental techniques are becoming available, and improved analytical procedures are becoming feasible. Currently the field of fatigue crack-growth-rate (FCGR) testing is undergoing critical examination under the combined auspices of the ASTM Committee E-24 on Fracture Testing of Materials and the U.S. Air Force. The special Task Group (E24.04.01) on Fatigue Crack Growth Rate Testing has published a report [1] on an extensive interlaboratory (round-robin) program established to identify and characterize sources of variability and bias inherent in such testing. Crack-length determination is singled out as the prime source of variability. The optical measurement method is the one in most common use. Such visual determination is both time consuming and subject to operator bias.

An alternative method developed and verified by NRL, measurement of the crack-opening displacement (COD) and determination of crack length a from a normalized calibration curve of  $EB[COD]/P$  vs  $a/W$ , has been used reliably for determining crack growth in thin-sheet plane-stress  $K_c$  specimens [2]. To assess its potential for crack-length measurement in FCGR testing, a suitable calibration curve was developed for the ASTM E24.04 compact tension (CT) specimen [3] and evaluated as successful for FCGR testing [4].

The evaluation was conducted on three materials: a 5Ni-Cr-Mo-V steel extensively studied in this laboratory; the 10Ni steel used in the ASTM E24.04.01 Task Group studies; and a 2024-T3 aluminum alloy. Crack-length determination was made from graphical analysis of the traces of load  $P$  vs COD produced by signals from both the load cell of the testing machine and the clip-gage circuit which were fed into an XY recorder.

However, the COD gage millivolt output is available for implementing the increasing trend towards automation. With confidence developed in the basic COD method of crack-length determination, a series of tests was performed so that the previously verified graphical method of data analysis could be compared to a potentially superior method using selected readings of millivolt output from the COD gage.

---

Note: Manuscript submitted October 14, 1975.

## EXPERIMENTAL CONSIDERATIONS

## Material

The 5Ni-Cr-Mo-V steel used for these tests is the same as that used for the evaluation studies [4]. Details of composition, heat treatment, and mechanical properties are to be found in Tables 1 and 2.

Table 1a — Composition of 5Ni-Cr-Mo-V Steel

Element	C	Ni	Cr	Mo	V	Al	Mn	P	S	Si	Fe
Percentage	0.11	4.85	0.58	0.48	0.07	0.01	180.87	0.002	0.005	0.30	Balance

Table 1b — Heat Treatment (HT)

Normalized:	1640°F; 1-1/2 hr; water quench
Austenitized:	1525°F; 1-1/2 hr; water quench
Tempered:	1050-1130°F; 1-1/2 hr; water quench
Stress Relieved (SR):	1000°F; 30 min; air cool

Table 2 — Mechanical Properties of Heat-Treated 5Ni-Cr-Mo-V Steel

Property	Value	
	Longitudinal	Transverse
Yield strength (0.2% offset) (ksi)	142	147
Tensile strength (ksi)	152	152
Elongation (%)	20	18
Reduction of area (%)	68	64

**Specimen Geometry**

The dimensions of the CT specimen (Fig. 1) conform to those selected for the ASTM E24.04.01 round-robin program [1]. However, to provide a longer fatigue crack extension beyond the machined notch, the initial notch length  $a_0$  was reduced from 0.700 to 0.500 in. (17.5 to 12.5 mm).

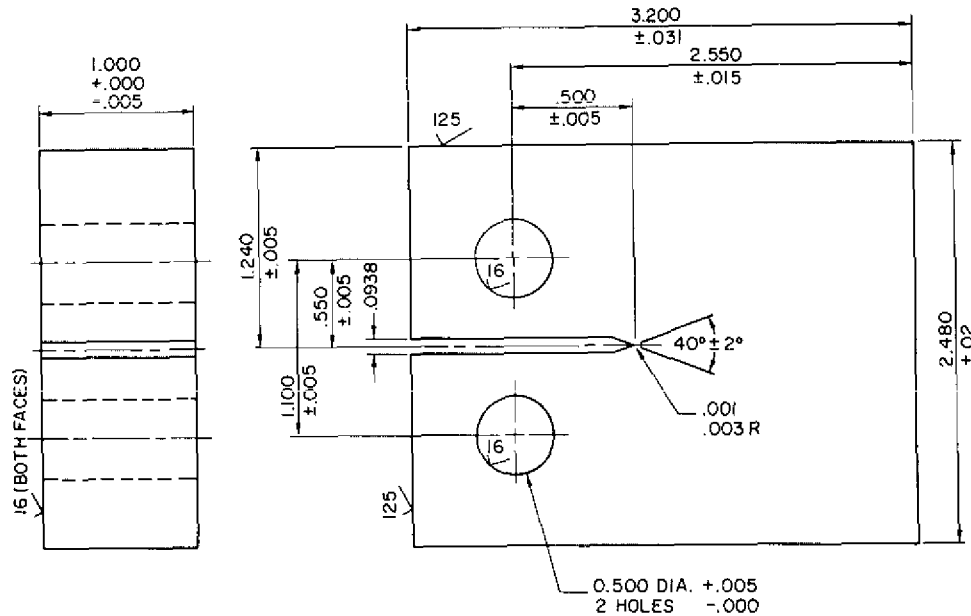


Fig. 1 — Compact tension specimen

**Test Procedure**

Specimens were cycled in tension-tension loading using a haversine waveform on a 110-kip-capacity MTS closed-loop testing machine. The cycle frequency was 5 Hz, and the stress ratio  $R$  was 0.10. Crack-length measurements were made using a COD technique [3, 4]. The COD measurements were obtained from a commercial MTS clip gage, the notched arms of which fit over knife edges screwed onto the specimen to straddle the mouth of the machined notch. Signals from the COD strain-gage circuit were fed to a Hewlett-Packard XY recorder together with those from the load cell of the testing machine. The COD strain-gage signals could also be read as millivolts on a digital voltmeter.

Excitation of the strain-gage circuit of the clip gage was provided by a Moxon 25-V power supply. Potentiometers in a balancing unit provided adjustments to both excitation voltage and COD output. Voltage was checked periodically and gage output adjusted (if necessary) to zero position before each reading. Tabulation of the exact procedural technique follows:

1. Equipment is turned on and given a warmup time of 30 to 60 min.
2. Excitation voltage is checked.
3. Gain settings are established for the XY recorder.
4. Gage is calibrated by means of an Instron high-magnification extensometer calibrator fitted with knife edges to accomodate the gage tips. The gage is nulled for calibration.
5. Gage is attached to the specimen and again nulled.
6. Initial cyclic interval is decided and preset.
7. When the preset cycles are accomplished, the machine automatically stops.
8. Gage is checked at zero load and the output nulled if necessary.
9. Specimen is loaded by operator manipulation of the loading dial. The gage output in mV is read at selected intervals of rising load and recorded. At the same time, a P-vs-COD trace is produced on the XY recorder.
10. For estimative purposes, the difference between the final two mV readings is used to determine crack length.
11. When intervals of crack growth become greater than about 0.025 in. (0.635 mm), the cyclic preset interval is reduced appropriately.
12. Approximate crack length vs number of cycles N can be plotted, if desired, to follow the data trend.
13. The test is terminated at an estimated crack length of about  $a/W = 0.56$  to 0.58.

#### Data Reduction

Crack length is provisionally determined from a graph of mV vs crack length appropriate to the specimen thickness. This graph is produced from known values of  $EB [COD]/P$  at various crack length-to-width ratios  $a/W$ :

$$\frac{EB[COD]}{P} = A, B, C, \text{ etc.};$$

$$\frac{COD}{P} = \frac{1}{EB} (A, B, C, \text{ etc.}) \text{ vs. } \frac{a}{W} \times W;$$

$$\text{COD} = \frac{P}{EB} (A, B, C, \text{etc.});$$

Therefore,  $mV = \text{COD}/\text{calibration factor}$  (determined from the gage output).

More accurate crack-length determination is achieved by converting mV readings to  $EB[\text{COD}]/P$  and determining  $a/W$ ; thus from the polynomial expression [3],

$$\begin{aligned} \frac{a}{W} = & 0.01520 \frac{EB[\text{COD}]}{P} - 0.000141 \left( \frac{EB[\text{COD}]}{P} \right)^2 \\ & + 0.000000524 \left( \frac{EB[\text{COD}]}{P} \right)^3 - 0.06209. \end{aligned} \quad (1)$$

Graphical determination of  $EB[\text{COD}]/P$  is also employed. This technique has been described in detail elsewhere [4].

Crack-growth rate was determined by fitting tangents to the  $a$ -vs- $N$  curves using a Bausch and Lomb split-prism tangent meter.

The stress-intensity-factor range  $\Delta K$  is computed from the equation appropriate to the half-height-to-width ratio  $h/W$  of the specimen [5]. For this specimen,  $h/W = 0.486$ , and

$$\Delta K = \Delta \sigma \sqrt{aY}, \quad (2)$$

where

$$\begin{aligned} Y = & 30.95 - 195.8 \frac{a}{W} + 730.6 \left( \frac{a}{W} \right)^2 \\ & - 1186.3 \left( \frac{a}{W} \right)^3 + 754.6 \left( \frac{a}{W} \right)^4. \end{aligned} \quad (3)$$

## DISCUSSION OF EXPERIMENTAL RESULTS

The fact that this series of tests had an alternative purpose, that of examining the effect of thickness on FCGR testing, is not relevant to this report. Suffice it to say that an effect of thickness was noted in material cut down from an as-heat-treated 0.90-in. (22.5-mm) plate. When stress relieved, the effect of thickness disappeared, but growth was seen to have accelerated. Full details of these results appear elsewhere [6].

Since the COD gage produces an analog signal well adapted for incorporation in the computerized automated procedures which are rapidly supplanting operator-run equipment, comparison of crack length and  $da/dN$  values determined from graphical analysis of the COD strain-gage signal vs selected millivoltage readings was deemed a useful investigation.

The first series of tests on an as-heat-treated material was run at different gain values on the XY recorder, and millivolt readings were taken only for the maximum load. When examining the P-vs-COD traces obtained from these tests, a nonlinearity was found to appear as soon as crack growth initiated, which became more pronounced with reduced specimen thickness. An example of this is seen in Fig. 2 for the stress-relieved material, where constant values for load and COD were used for all thicknesses.

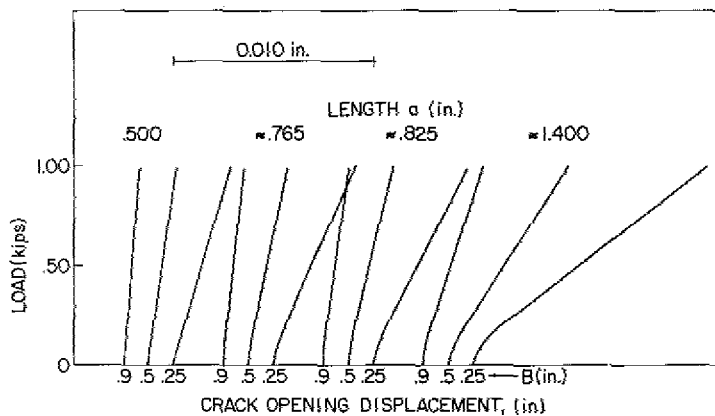


Fig. 2 — Load-vs-COD traces from compact tension specimens of three thicknesses of stress-relieved 5Ni-Cr-Mo-V steel

This nonlinearity had been observed previously in measurement of crack length by a similar COD technique in thin-sheet material. Compensation is made by drawing a "best fit" straight line through the data, as seen in Fig. 3. No compensation, of course, is made when following the procedure of simply using the mV output at maximum load. The effect of this can be seen in Figs. 4 and 5. The two specimens tested at two different loads to give an overlap of  $\Delta K$  values do not join to give a common  $da/dN$ -vs- $\Delta K$  curve using the maximum mV measurement but do so when the crack-length determinations are obtained by graphical means.

An improvement in technique was employed for the next series of tests using stress-relieved material. Millivolt readings were taken at the one load value common to tests of all specimens (1 kip) and at several other load values. The difference between mV readings at the last two loads illustrated in Fig. 2 was evaluated to obtain the slope of the P-vs-COD trace. Distribution of data is seen in Table 3.

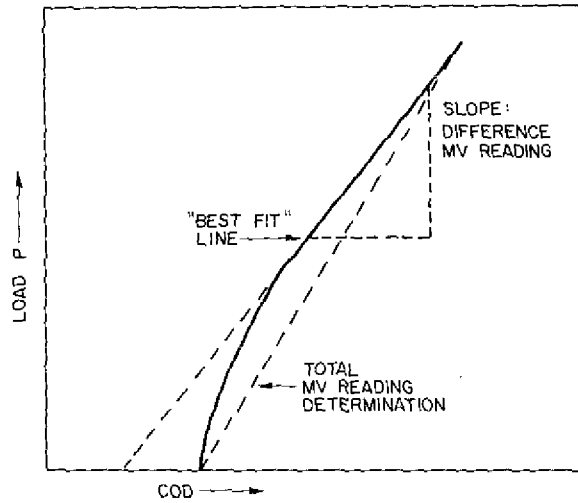


Fig. 3 — Load vs crack-opening displacement showing initial nonlinearity of the XY trace

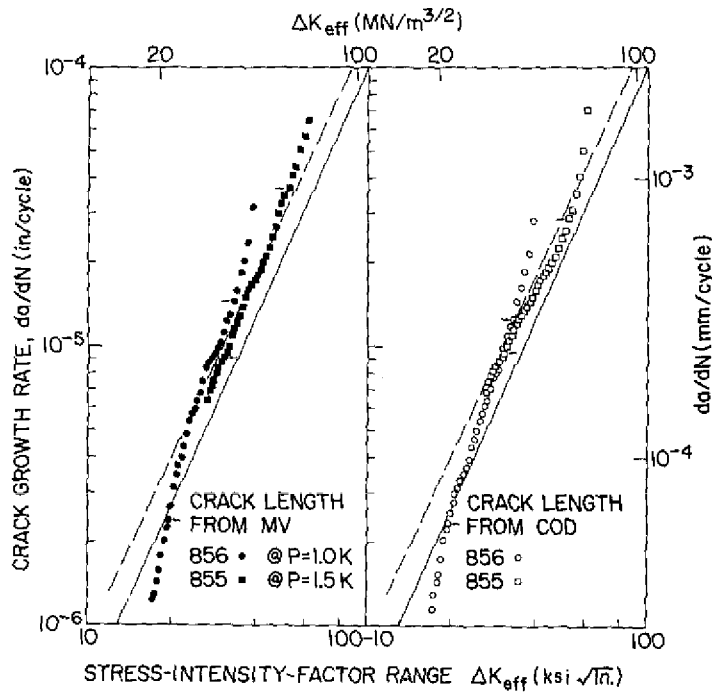


Fig. 4 — Crack-growth rate  $da/dN$  vs  $\Delta K_{eff}$ ; 5Ni-Cr-Mo-V steel as heat treated:  $B = 0.25$  in. (6.35 mm). The solid line represents the regression curve for the heat-treated 0.90-in. (22.5-mm) material; the dashed line represents the regression curve for all three thicknesses of the stress-relieved material.

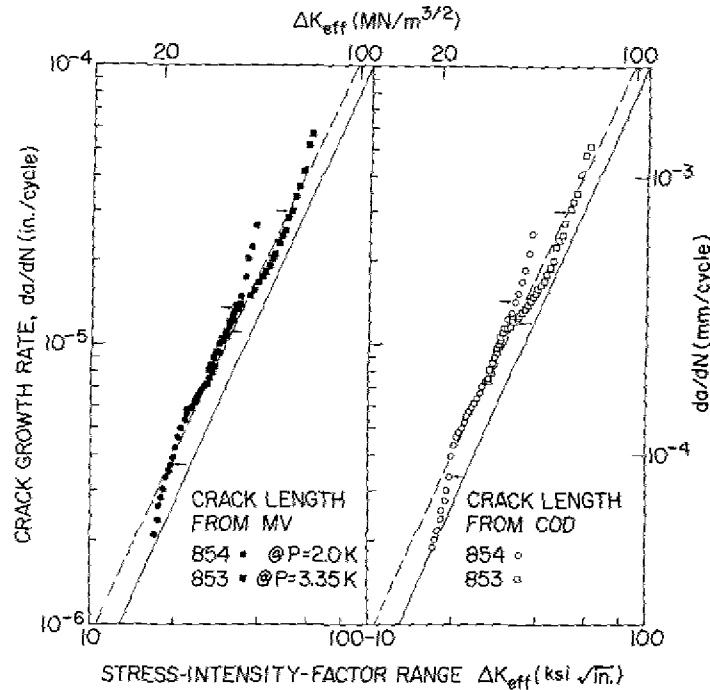


Fig. 5 — Crack-growth rate  $da/dN$  vs  $\Delta K_{eff}$ ; 5Ni-Cr-Mo-V steel as heat treated:  $B = 0.50$  in. (12.5 mm). The solid line represents the regression curve for the heat-treated 0.90-in. (22.5-mm) material; the dashed line represents the regression curve for all three thicknesses of the stress-relieved material.

In Figs. 6, 7, and 8, comparison is seen between  $da/dN$  vs  $\Delta K_{eff}$  when  $a$  is determined from mV readings at 1 kip and from the graph of  $P$  vs COD. Crack growth is faster in the former instance, but because all data are taken at the same load value, data from the two specimens provide a common curve.

Table 4 gives some details of crack-length-measurement comparison. In the stress-relieved material, optical, graphical COD, and mV-difference crack-length measurements agree quite well. For the heat-treated material, where crack length considerably exceeds 1.400 in. (35.6 mm), poor agreement is obtained between optical and graphical COD measurement. Departures from linearity apparently unrelated to the material have previously been noted [4] when the crack length is greater than 1.400 in. (35.6 mm).

Crack-length measurements from difference mV readings agreed well with graphical COD determination. Crossplots of  $a_{COD}$  and  $a_{mV}$  (Figs. 9 and 10) indicate the general trend of these relationships. Similar plots from all specimens tested give a relationship between  $a_{COD}$  and  $a_{mV}$  such that  $a_{COD} \approx a_{mV} + 0.05$ . FCGR tests on other materials, particularly titanium alloys, have shown an even more marked initial nonlinearity. Described as fatigue crack closure [7, 8] and observed in FCGR testing of sheet aluminum, it has been attributed to permanent tensile plastic deformations left in the wake of the propagating crack.

Table 3 - Details of the mV Readings

Specimen Number	Thickness B (in.)	Load Maximum on the Graph (kips)	mV Read at Indicated Load in kips						Difference (kips)
<b>As Heat Treated</b>									
856	0.25	1.00	—	1.0	—	—	—	—	—
855	0.25	1.50	—	—	1.5	—	—	—	—
854	0.50	2.00	—	—	—	2.0	—	—	—
853	0.50	3.50	—	—	—	—	3.5	—	—
844	0.90	4.00	—	—	—	—	—	—	—
845	0.90	4.00	—	—	—	—	—	—	—
847	0.90	9.76	—	—	—	—	—	—	—
<b>As Stress Relieved</b>									
858	0.25	1.00	0.5	1.0	—	—	—	—	1.0 - 0.5
860	0.25	1.50	0.5	1.0	1.5	—	—	—	1.5 - 1.0
863	0.50	2.00	—	1.0	—	2.0	—	—	2.0 - 1.0
861	0.50	3.00	—	1.0	—	2.0	3.0	—	3.0 - 2.0
859	0.90	2.00	—	1.0	—	2.0	—	4.0	4.0 - 2.0
862	0.90	4.00	—	1.0	—	2.0	—	4.0 6.0	6.0 - 4.0

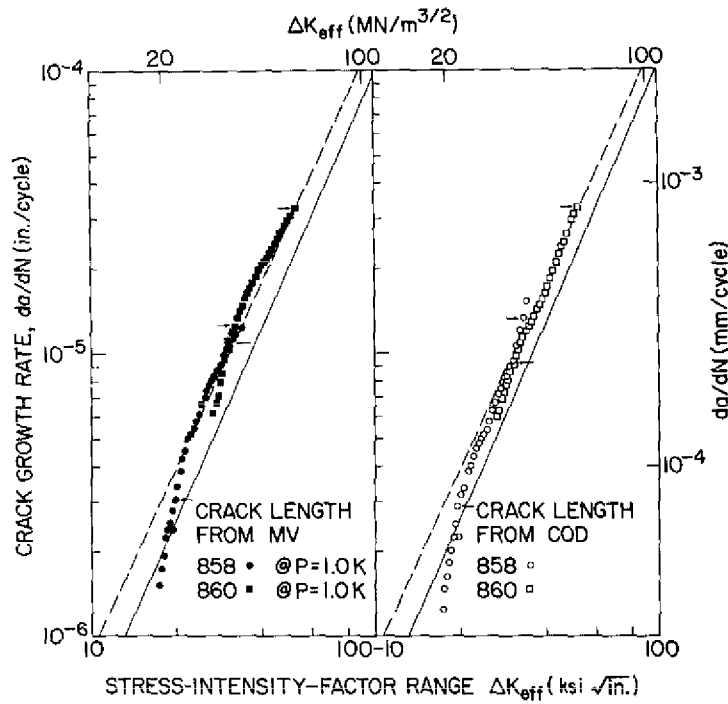


Fig. 6 - Crack-growth rate  $da/dN$  vs  $\Delta K_{eff}$ ; 5Ni-Cr-Mo-V steel as stress relieved: B = 0.25 in. (6.35 mm). The solid line represents the regression curve for the heat-treated 0.90-in. (22.5-mm) material; the dashed line represents the regression curve for all three thicknesses of the stress-relieved material.

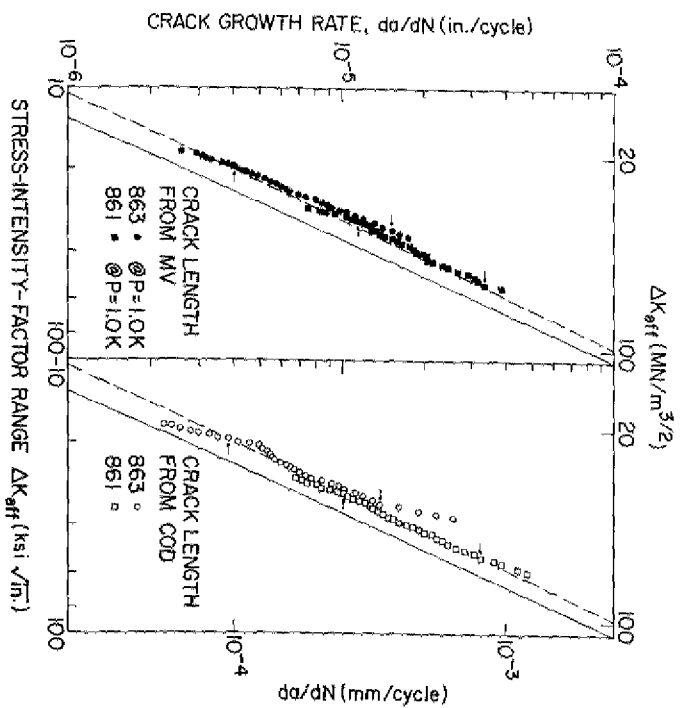


Fig. 7 — Crack-growth rate  $da/dN$  vs  $\Delta K_{eff}$ ; 5Ni-Cr-Mo-V steel as stress relieved;  $B = 0.50$  in. (12.5 mm). The solid line represents the regression curve for the heat-treated 0.90-in. (22.5-mm) material; the dashed line represents the regression curve for all three thicknesses of the stress-relieved material.

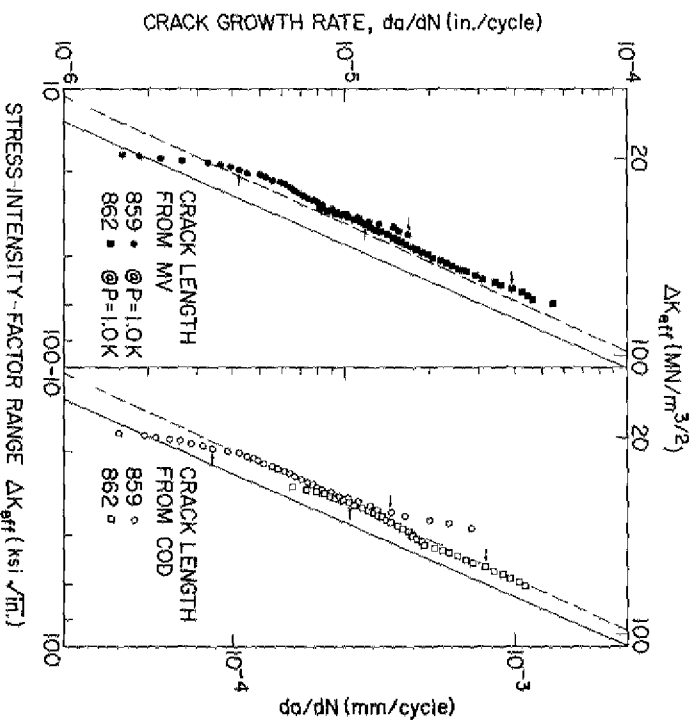


Fig. 8 — Crack-growth rate  $da/dN$  vs  $\Delta K_{eff}$ ; 5Ni-Cr-Mo-V steel as stress relieved;  $B = 0.90$  in. (22.5 mm). The solid line represents the regression curve for the heat-treated 0.90-in. (22.5-mm) material; the dashed line represents the regression curve for all three thicknesses of the stress-relieved material.

Table 4 — Details of the Crack-Growth Tests

Specimen Number	Thickness B (in.)	Hardness $R_c$		$\Delta P$ (kips)	$\Delta \sigma$ (ksi)	$a_0^*$ (Optical) (in.)	$a_f^\dagger$ (in.)				
		HT	SR				Optical	COD	mV @ $P_{diff.}$	mV @ $P_{max.}$	mV @ $P_{1K}$
As-Heat Treated											
856	0.25	—	—	1.11	1.74	0.4994	1.5841	1.956	—	1.62	—
855	0.25	—	—	1.74	2.74	0.5038	1.5957	1.787	—	1.69	—
854	0.50	—	—	2.22	1.74	0.4992	1.5625	1.660	—	1.60	—
853	0.50	—	—	3.48	2.74	0.5010	1.5259	1.612	—	1.58	—
844	0.90	—	—	4.04	1.74	0.4848	1.5931	1.530	—	—	—
845	0.90	—	—	4.04	1.74	0.4956	1.6138	1.792	—	—	—
847	0.90	—	—	9.76	4.25	0.4874	1.5963	1.686	—	—	—
As-Stress Relieved											
858	0.25	34.8	34.4	1.11	1.74	0.5032	1.4260	1.424	1.431	1.380	1.380
860	0.25	33.8	33.6	1.74	2.74	0.5012	1.4355	1.394	1.444	1.397	1.374
863	0.50	—	—	3.48	1.74	0.5037	1.4657	1.461	1.475	1.454	1.433
861	0.50	32.7	34.6	3.48	2.74	0.5021	1.4600	1.474	1.470	1.442	1.402
859	0.90	34.6	34.2	4.04	1.74	0.4911	1.4736	1.483	1.494	1.474	1.424
862	0.90	34.8	35.3	6.28	2.74	0.4957	1.4903	1.544	1.526	1.507	1.438

\*Initial

†Final

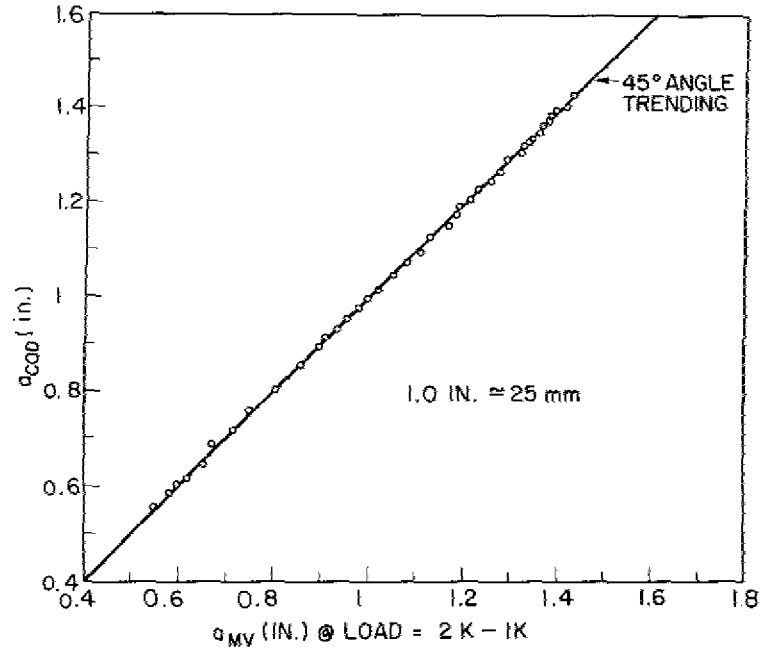


Fig. 9 — Crossplot of crack length measured graphically,  $a_{COD}$ , and from difference mV readings,  $a_{mv}$ . Good agreement is evident.

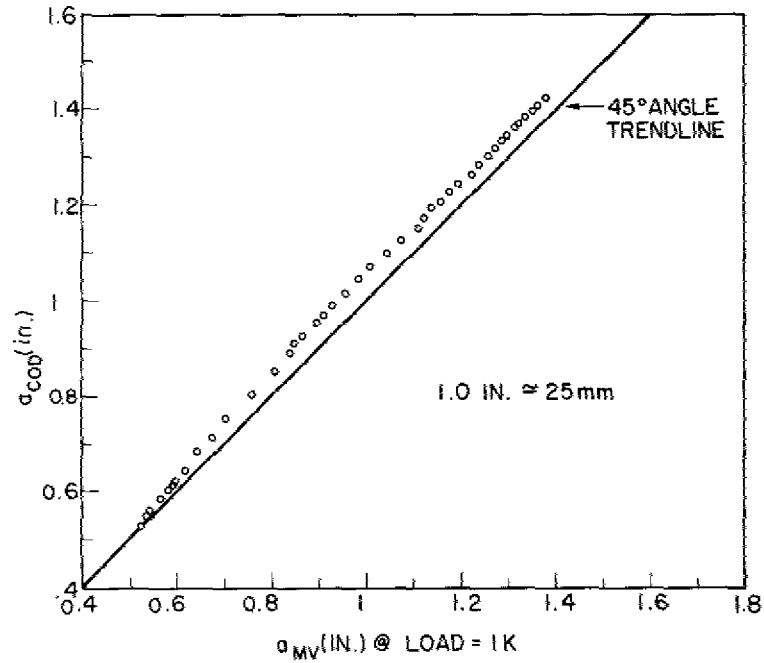


Fig. 10 — Crossplot of crack length measured graphically,  $a_{COD}$ , and from total mV reading at  $P = 1K$ ,  $a_{mv}$ . Shorter crack lengths are indicated by the mV readings.

Another possible source for this initial nonlinearity may lie in the disparate widths of the machined notch and "natural" fatigue crack. Similar specimens tested with (a) the total crack length machined and (b) the total crack length fatigued indicate greater crack opening for the total fatigue crack [9].

For these reasons, it is at present difficult to suggest a standard method of data collection which would insure that mV readings were taken at appropriate intervals of loading. Possibly a series of readings could be taken at increasing load levels until constant difference values were attained. Alternately, one might always take a difference between  $P_{\text{final}}$  and  $P_{\text{final}} - 0.5K$  or  $1K$ . The low loads required by the CT specimen contribute to the difficulty.

## CONCLUSIONS

- To compensate for nonlinearity in the load-vs-COD traces, incremental differences in the load millivolt readings must be sampled.
- Millivolt readings at peak loads for a series of specimens at varied loads will not produce a smooth  $da/dN$ -vs- $\Delta K$  curve.
- If mV readings are taken at the same low load for a series of tests at increasing loads, the  $da/dN$  curve will indicate growth rates in excess of the actual growth rates.

## ACKNOWLEDGMENT

The assistance provided by Messrs. G.W. Jackson and M.L. Cigledy in performing this experimental work is gratefully acknowledged by the author.

## REFERENCES

1. W.G. Clark, Jr., and S.J. Hudak, Jr., "Variability in Fatigue Crack Growth Rate Testing — an ASTM E24.04.01 Task Group Report," Westinghouse Research Laboratories, Pittsburgh, PA, Scientific Paper 74-1E7-MSLRA-P2 (1974).
2. A.M. Sullivan and C.N. Freed, "A Review of the Plane-Stress Fracture Mechanics Parameter  $K_c$  Determined Using the Center-Cracked Tension Specimen," NRL Report 7460, Dec. 29, 1972.
3. A.M. Sullivan, "Crack Length Determination for the Compact Tension Specimen Using a Crack-Opening-Displacement Calibration," NRL Report 7888, June 24, 1975.
4. A.M. Sullivan and T.W. Crooker, "Evaluation of Fatigue Crack-Growth-Rate Determination Using a Crack-Opening-Displacement Technique for Crack-Length Measurement," NRL Report 7912, Sept. 12, 1975.

5. E.T. Wessel, "State of the Art of the WOL Specimen for  $K_{Ic}$  Fracture Toughness Testing," *Engineering Fracture Mechanics* 1, 77 (1968).
6. A.M. Sullivan and T.W. Crooker, "Effect of Specimen Thickness on Fatigue Crack-Growth Rate in 5Ni-Cr-Mo-V Steel — Comparison of Heat-Treated and Stress-Relieved Specimens," NRL Report 7936 (publication pending).
7. W. Elber, "Fatigue Crack Closure Under Cyclic Tension," *Engineering Fracture Mechanics* 2, 37 (1970).
8. W. Elber, "The Significance of Fatigue Crack Closure," in *Damage Tolerance in Aircraft Structures*, ASTM STP 486, Philadelphia, p. 230, 1971.
9. G.R. Yoder and C.A. Griffis, "Influence of Calibration Procedure Upon Determination of  $J_{Ic}$  for a Titanium 6Al-4V Alloy," NRL Report 7710, Apr. 30, 1974.